Journal of Power Sources 195 (2010) 6130–6137

Contents lists available at ScienceDirect

Journal of Power Sources

journal homepage: www.elsevier.com/locate/jpowsour

UV cross-linked, lithium-conducting ternary polymer electrolytes containing ionic liquids

G.T. Kim[a], G.B. Appetecchi[a,**], M. Carewska[a], M. Joost[b], A. Balducci[b], M. Winter[b], S. Passerini[a,b,*]

[a] ENEA, IDROCOMB, Casaccia Research Center, Via Anguillarese 301, 00123 Rome, Italy
[b] Institute of Physical Chemistry, University of Muenster, Corrensstr. 28/30, D 48149 Muenster, Germany

ARTICLE INFO

Article history:
Received 24 September 2009
Received in revised form 25 October 2009
Accepted 29 October 2009
Available online 10 November 2009

Keywords:
Polymer electrolyte
Lithium batteries
Ionic liquid
PEO
LiTFSI
UV cross-linking

ABSTRACT

In this manuscript is reported an attempt to prepare high ionic conductivity lithium polymer electrolytes by UV cross-linking the poly(ethyleneoxide) (briefly called PEO) polymer matrix in presence of the plasticizing lithium salt, lithium bis(trifluoromethanesulfonyl)imide (LiTFSI) and an ionic liquid of the pyrrolidinium family (*N*-alkyl-*N*-methylpyrrolidinium TFSI) having a common anion with the lithium salt. It is demonstrated that polymer electrolytes with room temperature ionic conductivities of nearly 10^{-3} S cm^{-1} could be obtained as a result of the reduced crystallinity of the ternary electrolytes. The results clearly indicate that the cross-linked ternary electrolyte shows superior mechanical properties with respect to the non-cross-linked electrolytes and higher conductivities with respect to polymer electrolytes containing none or less ionic liquid.

1. Introduction

Rechargeable lithium batteries outpaced all other battery systems in the consumer portable electronic and telecommunications markets within the last few years. However, to power the hybrid and/or pure electric vehicles of tomorrow, lithium batteries have to provide even higher energy and/or higher power densities, better cyclability, reliability, and, overall, safety. Lithium metal batteries with their theoretically high gravimetric energy and power densities are a desired solution. However, the liquid organic electrolytes that have warranted the great success to present lithium-ion batteries, appears to be not useful because of their high reactivity with Li-metal that results in poor performance and uneven (dendritic) anode deposition. This latter phenomenon raises serious safety issues considering that the conventional electrolytes for Li-ion batteries are mostly composed of volatile flammable solvents, which could easily cause fire or explosion of the battery upon dendritic short-circuit. Actually, the safety issue caused by the electrolytes' fire and explosion hazards is indeed present in large Li-ion batteries and, so far, it has prevented the wide deployment of Li-ion batteries in hybrid and electric vehicles. The thermal runaway of a Li-ion battery is a catastrophic, uncontrollable event that occasionally happens even in long established applications such as laptop PC and cell phones [1].

Lithium metal, polymer electrolyte batteries (LMPBs) have been proposed since early 1980s as the solution to the safety issues. So far, however, LMPBs are substantially limited to high-temperature operations since solvent-free polymer electrolytes, such as those with dissolved lithium salt in poly(ether/glycols), are characterized by a relative low ionic conductivity at room temperature.

Most of the work on polymer electrolytes, so far, has been focusing on poly(ethylene oxide) (PEO). PEO is an inert polymer and its application as electrolyte host has been intensively studied for almost four decades now [2]. The fact that PEO builds complexes with Li salts and displays both thermal and interfacial stabilities [3] makes it a promising candidate as polymer electrolyte host. However, at room temperature the ionic conductivity of Li salts dissolved in PEO is limited because the highly symmetrical repeating ethylene oxide units tend to crystallize. Amorphous areas are necessary for sufficient ionic conductivity [4,5]. Li salts with large anions free the Li^+ from the strong EO coordination. An ionic liquid as additional salt, providing the same anion seems to promote this process and the voluminous cations create "free-volume" [6,7] for diffusion. Recently, the combination of a polymer and an ion conducting, electrochemically stable ionic liquid has been explored as a polymer-based electrolyte in lithium ion batteries [8]. A broad and stable amorphous region of PEO was created. Ionic liquids are perfectly suitable for battery applications, because they present high

* Corresponding author. Tel.: +49 251 83 36026; fax: +49 251 8336032.
** Corresponding author. Tel.: +39 06 3048 4985; fax: +39 06 3048 6357.
E-mail addresses: gianni.appetecchi@enea.it (G.B. Appetecchi), stefano.passerini@uni-muenster.de (S. Passerini).

0378-7753/$ – see front matter © 2009 Elsevier B.V. All rights reserved.
doi:10.1016/j.jpowsour.2009.10.079

Table 1
Electrochemical properties of cross-linked PEO–LiTFSI–$PYR_{14}TFSI$ polymer electrolytes processed at different UV photo-irradiation times.

Irradiation time (min)	Conductivity ($mS\,cm^{-1}$)		Interfacial resistance at 20 °C ($\Omega\,cm^2$)	
	20 °C	40 °C	Fresh cell	After 1 month
3	0.37 ± 0.03	1.2 ± 0.1	1300 ± 100	2500 ± 200
5	0.34 ± 0.02	1.1 ± 0.1	1300 ± 100	2500 ± 200
7	0.32 ± 0.02	1.0 ± 0.1	1200 ± 100	2200 ± 200
9	0.33 ± 0.02	1.0 ± 0.1	1200 ± 100	2700 ± 200

chemical and thermally stability, negligible vapour pressure, non-flammability and in some cases high electrochemical stability and hydrophobicity [9–12].

The ionic liquid *N*-methyl-*N*-butylpyrrolidinium bis(trifluoromethansulfonyl)imide ($PYR_{14}TFSI$) [13] and lithium bis(trifluoromethansulfonyl)imide (LiTFSI) as conducting salt are used in this work [14–16]. The membranes are easily prepared by a solvent-free technique in which the components are mixed together and hot pressed, a considerably more attractive preparation procedure for industrial applications than the typically used solvent-casting. The resulting PEO–RTIL–LiTFSI materials are true dry solid polymer electrolytes (SPE) consisting solely of commercial high molecular weight PEO and two salts.

Conductivities of about $10^{-4}\,S\,cm^{-1}$ at or near ambient temperature are needed to match the requirements for application in batteries for electronic devices and electric vehicles [17]. The ionic conductivity of the new SPE is almost two orders of magnitude higher than that of ionic-liquid-free PEO–LiTFSI electrolyte [8] and if the PEO/IL/LiTFSI ratio is increased from 10/1/1 (by mole) to 10/2/1, the ionic conductivity is further increased, from $10^{-4}\,S\,cm^{-1}$ to $3 \times 10^{-4}\,S\,cm^{-1}$ at 20 °C. Unfortunately, the mechanical stability of the electrolyte membrane suffers at increasing IL content, where sticky materials are obtained. In the attempt to obtain room temperature highly conductive polymer electrolytes without depleting their mechanical properties, we have "in situ" UV photo-irradiated the PEO chains, in presence of LiTFSI and $PYR_{14}TFSI$, to obtain chemically cross-linked membranes. UV-induced cross-linking of the PEO chains was performed with benzophenone (Bp) as cross-linking agent thus allowing to obtain processable thin polymer films.

This work is a contribution to the development of safe lithium batteries, which can be operated without the use of volatile and combustible electrolyte liquids.

2. Experimental

2.1. Synthesis of the ionic liquids

The $PYR_{14}TFSI$ ionic liquid was synthesized through a procedure developed at ENEA and described in details elsewhere [13]. The chemicals *N*-methylpyrrolidine (ACROS, 98 wt.%) and 1-bromobutane (Aldrich, 99 wt.%) were previously purified through carbon and alumina before the synthesis process. LiTFSI salt (3 M, 99.9 wt.%), activated carbon (Aldrich, Darco-G60), alumina (Aldrich, acidic, Brockmann I) and ethyl acetate (Aldrich, >99.5 wt.%) were used as received.

2.2. Preparation of cross-linked ternary solid polymer electrolytes and composite cathodes

A solvent-free, hot-pressing process developed at ENEA [3,18] was followed to prepare the cross-linked PEO–LiTFSI–$PYR_{14}TFSI$ ternary solid polymer electrolytes and the composite cathodes. The process was performed in a very low relative humidity dry room (RH < 0.2% at 20 °C). For the electrolyte samples, LiTFSI (3 M, 99.9 wt.%) and the $PYR_{14}TFSI$ ionic liquid were dried under vacuum at 120 °C for at least 18 h before use while poly(ethylene oxide) (Dow Chemical, WSR 301, M_W = 4,000,000), was dried at 50 °C for 48 h. Benzophenone (Aldrich) was used (as received) as initiator for the cross-linking process. The Bp/PEO weight ratio was kept equal to 0.05 [19] while the $(PYR_{14})^+/Li^+$ mole ratio was fixed equal to 2. First, Bp was dissolved in $PYR_{14}TFSI$ at 80 °C under vacuum for one day. PEO and LiTFSI (EO/Li mole ratio = 10) [16] were mixed in a mortar and, then, added to the Bp/$PYR_{14}TFSI$ solution. After complete blending, the PEO–LiTFSI–$PYR_{14}TFSI$–Bp mixture was annealed under vacuum at 100 °C for 2–3 days to obtain a homogeneous, plastic-like material. The latter was sandwiched between two Mylar foils and, then, hot-pressed at 70 °C and 180 $kg\,cm^{-2}$ for 7–8 min to obtain 0.1 mm thick films. Finally, the polymer electrolyte tapes were cross-linked by a UV Karl-Suss MA 45 photo-irradiator (with a 350 W Hg lamp) for time periods ranging from 3 min to 11 min.

Cross-linked composite cathode tapes were prepared by intimately mixing $LiFePO_4$ (active material synthesized by Süd Chemie, 43 wt.%) and carbon (KJB, Akzo Nobel, 7 wt.%), which were previously dried in a vacuum oven at 120 °C for at least 24 h. PEO (17.5 wt.%), LiTFSI (5.0 wt.%) and $PYR_{14}TFSI$ (27.5 wt.%) and Bp (5 wt.% of PEO) were separately mixed to obtain a paste-like mixture that was added to the previous $LiFePO_4$/C blend. The final cathodic mixture was firstly annealed at 100 °C overnight and, then, cold-calendered to form 0.05 mm thick cathode films. Finally, the cathode tapes were UV photo-irradiated for 8 min (4 min on each side) by using a Karl-Suss MA 45 equipment.

2.3. Determination of water content

The water content in the ionic liquid, the lithium salt, the PEO and the non-cross-linked polymer electrolyte samples was measured using the standard Karl Fischer method. The titrations were performed with an automatic Karl Fischer coulometer titrator (Mettler Toledo DL32) located inside the dry room (RH < 0.2% at 20 °C). The Karl Fischer titrant was a one-component (Hydranal 34836 Coulomat AG) reagent provided from Aldrich. For all these materials the water content was always lower than 10 ppmw. The ionic liquid, in particular, contained less than 1 ppmw. The cross-linked solid polymer electrolyte samples were also tested but the results obtained were not reliable. In fact, the SPE did not dissolve in the analyte solution thus making the direct measurement impossible (no water was detected but it could depend on the low water release kinetic). In a second attempt, the cross-linked samples were heated ex situ under inert gas flow. However, the water release was too slow to allow detection. Unlikely, the process could not be accelerated by increasing the temperature without water release due to sample decomposition. In the final attempt, cross-linked samples were immersed in anhydrous ethanol to extract the water. The ethanol solutions were tested for water content before and after the extraction but the results (i.e., the difference in the water content before and after the extraction) appeared to be scattered and not reproducible. As a final conclusion we can comfortably state that the water content in the cross-linked SPE was lower than 20 ppmw.

2.4. Determination of cross-linked fraction

The cross-linked fraction in ternary polymer electrolytes was determined as described in the following. The electrolyte samples were weighed and subsequently extracted with acetonitrile, mostly to remove the lithium salt and the ionic liquid, and dichloromethane to extract the non-cross-linked PEO chains. Extraction included several hours of residence time for the solvents to appeal the SPE. The cross-linked fraction (W) was then calculated by dividing the mass of the dried sample left after the extraction by the calculated mass of PEO in the original sample [20].

2.5. Thermal analysis

Thermal measurements on the cross-linked PEO–LiTFSI–PYR_{14}TFSI ternary polymer electrolytes were performed using a TA Instruments (Model Q100) differential scanning calorimeter (DSC). Hermetically sealed Al pans were prepared in the dry room. Typically, the electrolyte samples were cooled at 20 °C min^{-1} from room temperature down to −140 °C and then heated at 10 °C min^{-1} up to 100 °C.

2.6. Test cells assembly

The conductivity, interfacial stability, lithium stripping-plating and linear sweep measurements on the cross-linked PEO–LiTFSI–PYR_{14}TFSI ternary solid polymer electrolytes were performed on sealed, laminated, two-electrode, pouch cells fabricated inside the dry room. The test cells were assembled by sandwiching a polymer electrolyte film between two copper (conductivity measurements; active area equal to 9 cm^2) or lithium foils (Li/polymer electrolyte interfacial stability and lithium stripping-plating measurements; active area equal to 1–2 cm^2) or between a nickel (linear sweep voltammetry tests, working electrode; 0.125 mm thick; active area equal to 1.0–1.5 cm^2) and a lithium foil (counter and reference electrode; 0.05 mm thick). The assembled cells were housed in sealed, coffee-bag envelopes and successively laminated twice by hot-rolling at 100 °C.

The solid-state Li/$LiFePO_4$ full batteries (cathode limited) were fabricated by laminating a lithium foil (50 μm thick), a cross-linked PEO–LiTFSI–PYR_{14}TFSI ternary solid polymer electrolyte membrane and a $LiFePO_4$-based composite cathode tape. The assembled cells were housed in sealed, coffee-bag envelopes and successively laminated twice by hot-rolling at 100 °C. The electrochemical active area of the laminated cells approached 1 cm^2. The active material mass loading approaches 4.5 mg cm^{-2}, corresponding to 0.76 mAh cm^{-2}.

2.7. Electrochemical tests

The ionic conductivity of the cross-linked PEO–LiTFSI–PYR_{14}TFSI ternary solid polymer electrolytes and their interfacial stability with lithium metal anode were determined by impedance measurements taken on Cu/SPE/Cu or Li/SPE/Li cells, respectively. The AC tests were performed by means of a Frequency Response Analyzer (F.R.A., Schlumberger Solartron 1260) in the 1 Hz to 100 kHz (conductivity tests) and 0.1 Hz to 65 kHz (interfacial stability tests) frequency ranges, respectively.

The conductivity tests were performed on a heating stepped ramp from −40 °C to 100 °C. Prior to perform the temperature ramp the Cu/SPE/Cu cells were held at −40 °C for 24 h to avoid slow kinetic effects on the polymer electrolytes. The temperature was changed in 10 °C steps every 24 h to allow a complete thermal equilibration of the cells before each measurement. The interfacial stability measurements were taken for a storage time exceeding 6 months during which the temperature was changed to investigate its effect on the Li/SPE interfaces. Initially, the cells were stored at 20 °C for 55 days. After this period, the storage temperature was increased to 80 °C for 40 days and, then, again reduced at 20 °C for additional 90 days. The test cells were located in a climate test chamber (Binder GmbH MK53) with a temperature control of ±1 °C.

The impedance responses were analyzed using the well-known Non-Linear Least-Square (NLLSQ) fit software on the basis of a suitable equivalent circuit model [21–23]. All measurements were carried out on at least three different cells for each SPE in order to verify the reproducibility of the obtained results.

The cyclability of lithium metal electrodes in cross-linked PEO–LiTFSI–PYR_{14}TFSI ternary solid polymer electrolytes was evaluated by stripping/plating tests on symmetric Li/SPE/Li two-electrode cells at 40 °C. The test consisted in flowing a constant current (0.078 mA cm^{-2}) through the cells, but its polarity was reversed every 1 h. The cyclability at the Li/SPE interface was followed by recording the cell overvoltage during the galvanostatic tests where each electrode alternatively acts as source and sink of lithium ions moving in the polymer electrolyte. These tests, performed using a Maccor S4000 battery cycler, are focused to evaluate the amount of lithium that is lost during the plating step and, therefore, the Li/SPE interface stability under current flow.

The electrochemical stability window of cross-linked PEO–LiTFSI–PYR_{14}TFSI ternary solid polymer electrolytes was evaluated by linear sweep voltammetries (LSVs) at 0.5 mV s^{-1}. Separate LSV tests were carried out on each polymer electrolyte sample to determine the cathodic and anodic electrochemical stability limits. The measurements were performed scanning the cell voltage from the open circuit value (OCV) towards more negative (cathodic limit) or positive (anodic limit) voltages. Clean electrodes and a fresh sample were used for each test. To confirm the results obtained the LSV tests were performed at least twice on different fresh samples of each cross-linked PEO–LiTFSI–PYR_{14}TFSI material, respectively. The measurements were performed at 20 °C and 40 °C using an Schlumberger (Solartron) Electrochemical Interface (model 1287) controlled by a software developed at ENEA.

Preliminary cycling tests on full Li/$LiFePO_4$ polymer batteries were performed at temperatures ranging from 20 °C to 40 °C using a MACCOR S4000 battery tester. The voltage cut-offs were fixed at 4.0 V (charge step) and 2.0 V (discharge step), respectively.

3. Results and discussion

3.1. Mechanical properties

The mechanical properties of the cross-linked polymer electrolytes are quite exceptional. In the pictures of Fig. 1 it is shown that a small sample of cross-linked PEO–LiTFSI–PYR_{14}TFSI material can be stretched up to more than 20 times of its original length without breaking. Even more amazingly, the sample is elastomeric and gained its original shape after release. Nevertheless, samples with UV photo-irradiation times shorter than 7 min or higher than 14 min turned to be sticky and fragile. This bell-shape behavior is given by the balance among the UV photo-irradiation induced cross-linking and bond-cleavage (depolymerization). This was proved by the experiments for cross-linking fraction determination (see Fig. 2). Samples with irradiation times lower than 7 min turned to have low cross-linking rates (data not shown in Fig. 2). They were partly dissolved in the solvents and further extraction was impossible. The same was noticed for samples with irradiation times longer than 14 min. UV photo-irradiation from two sides resulted in a more effective cross-linking with better reproducibility. Considering the low (not determinable) cross-linking fractions at long and short UV photo-irradiation times, cross-linking fraction vs. irradiation time

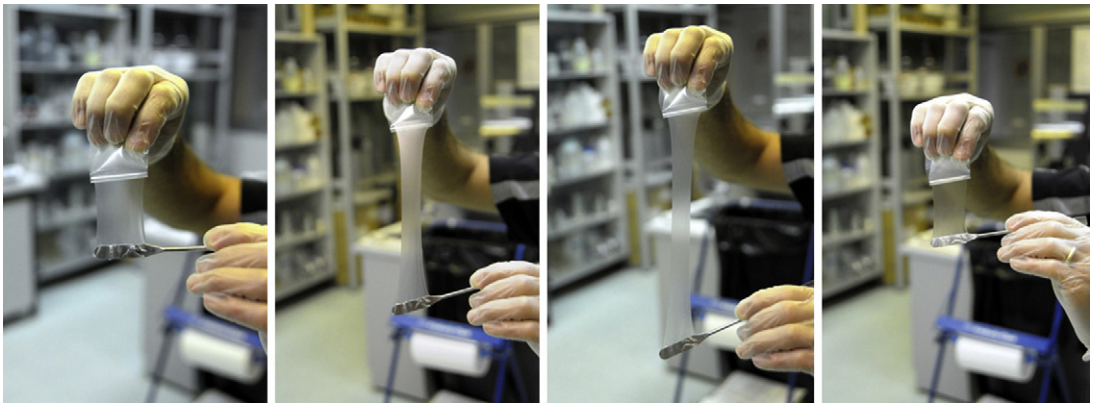

Fig. 1. Cross-linked PEO–LiTFSI–$PYR_{14}TFSI$ ternary polymer electrolyte sample (UV photo-irradiation time was 9 min) subjected to manual elongation.

can be considered as Gaussian-like with a maximum at around 12–13 min.

3.2. Thermal properties

Fig. 3A illustrates the DSC measurements performed on PEO–LiTFSI–$PYR_{14}TFSI$ solid polymer electrolyte samples synthesized with different cross-linking times. For comparison, the DSC traces of a Bp-free sample and a not irradiated sample were also taken. A very uniform behavior is observed. The glass-transition temperature (T_g), originally −54 °C in pure PEO [24] is seen for all samples at around −67 °C confirming that the addition of the two salts decreases the T_g of PEO, as expected from a salt incorporation into the polymer. However, the typical peaks observed in PEO–LiX binary mixtures [25–27], corresponding to the melting of the $P(EO)_6$–LiTFSI crystalline phase and the pure PEO phase, do not appear in the DSC traces. This effect was already reported in similar, not cross-linked, ternary polymer electrolytes [28]. It was proposed that due to the strong interaction taking place among the lithium salt, the ionic liquid and the polymer, the formation of polymer-containing crystalline phases is prevented [8,16]. The peaks appearing around 15 °C and 25 °C in the cross-linked and non-cross-linked samples, respectively, is most likely due to the melting of some excess LiTFSI–$PYR_{14}TFSI$ phase as reported earlier [8]. The shift of the peak upon cross-linking indicates a change of the composition of the excess LiTFSI–$PYR_{14}TFSI$ phase. The comparison with the phase diagram of the LiTFSI–$PYR_{14}TFSI$ system [14] indicates that this phase is enriched in its ionic liquid content. In addition, this peak disappeared in samples that have been stored in the sealed DSC pans outside the dry room for several hours prior to DSC measurements (see Fig. 3B and C). However, the disappearance of this peak was faster in non-cross-linked samples (Fig. 3B). While it is well known that the presence of humidity strongly affects the lithium coordination, making the observed peak vanishing possible, this evidence is rather important to prove the dryness of all SPE samples investigated in this work.

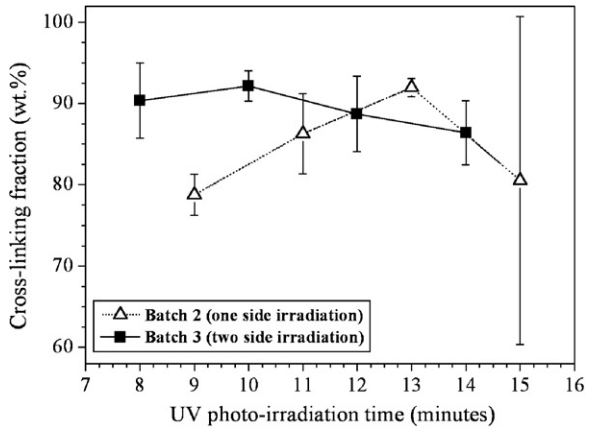

Fig. 2. Cross-linked polymer fraction as a function of the UV photo-irradiation time in cross-linked PEO–LiTFSI–$PYR_{14}TFSI$ ternary polymer electrolytes.

To summarize, the addition of $PYR_{14}TFSI$ effectively prevents crystallization of PEO and PEO–LiTFSI complexes. This assures a wide amorphous range of the polymer electrolyte, which is important for ionic conductivity. Cross-linking does not affect the thermodynamic behavior of the ternary system excluding a slight change of the excess LiTFSI–$PYR_{14}TFSI$ phase.

3.3. Ionic conductivity

The temperature dependence of the ionic conductivity is presented in Fig. 4A and Table 1. The incorporation of an ionic liquid into PEO polymer electrolytes increases the ionic conductivity (σ) dramatically, as it has been proved and discussed by Kim et al. [20]. Doubling the IL content from 10:1:1 to 10:2:1 (EO:IL:LiX) raises the RT conductivity from 10^{-4} S cm^{-1} to 3×10^{-4} S cm^{-1}. The interesting conductivity boarder of 10^{-3} S cm^{-1} is reached at 40 °C. The SPE exhibits a VTF like behavior [29], which stresses the presence of a fully amorphous phase. Cross-linking does not affect the conductivity at moderate or high temperatures; only at temperatures below zero a slight decrease in conductivity can be noticed at higher cross-linking times.

Larger IL/LiTFSI ratios do not result in much higher conductivities as it is seen in Fig. 4B. Doubling the IL content from 10:1:2 to 10:1:4 results in only doubling the ionic conductivity but this happens at the expenses of the mechanical properties which are much lower. The 10:1:4 material was very sticky and tended to break very easily on elongation.

3.4. Electrochemical stability window (ESW)

The electrochemical stability windows of the SPEs measured in Li/SPE/Ni cells at 20 °C and 40 °C, are depicted in Fig. 5. Independent on the cross-linking time, all materials exhibited a wide ESW ranging from the lithium plating to above 5.0 V vs. Li/Li^+ at room temperature and 4.8 V vs. Li/Li^+ at 40 °C. A few, rather small (less than 20 μA cm^{-2}), features are observed in the cathodic scans of all materials thus excluding their relation with benzophenone or the crosslinking process. In order to investigate the origin of these features, a cell was subjected to the consecutive cyclic voltammetric test (see Fig. 5C). From the trend of this test it is clearly seen that all features tend to decrease quite rapidly on cycling with peak

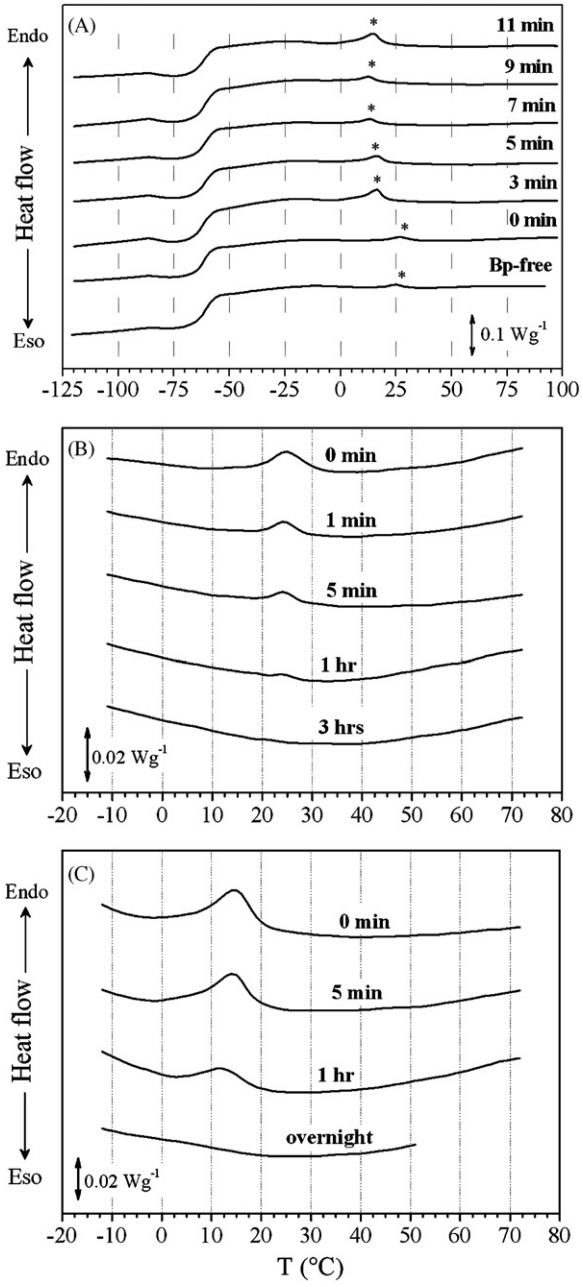

Fig. 3. DSC traces of cross-linked PEO–LiTFSI–PYR_{14}TFSI ternary polymer electrolytes at different UV photo-irradiation times (panel A). The thermal curve of the initiator-free polymer electrolyte is reported for comparison purpose. Panels B and C illustrate the evolution of the DSC peak of two samples (irradiation time of 0 min and 7 min, respectively) stored in sealed pans in ambient air. Scan rate: 10 °C min^{-1}. The asterisk marks the peak associated with the free LiTFSI–PYR_{14}TFSI phase.

currents as low as 3 μA cm^{-2} after only 10 CV cycles. Nevertheless, the peaks never disappeared completely thus indicating that some kind of reversible reaction took place in the cell. A literature search led to the identification of the peaks at 1.5 V and 0.5 V vs. Li/Li^+ with the more or less reversible Li insertion into the native NiO_x layer on the Ni electrode surface [30]. Calculations based on the total charge involved in the 1.5 V vs. Li/Li^+ peak indicate that a 4 nm layer of native NiO_x oxide would be present onto the nickel electrode, which is a very reasonable thickness for a native oxide layer on such a metal. The peak at 0.75 V vs. Li/Li^+ is probably due to LiTFSI impurities and maybe water contamination [11]. Reactions of benzophenone or generation of terminal active groups in PEO by

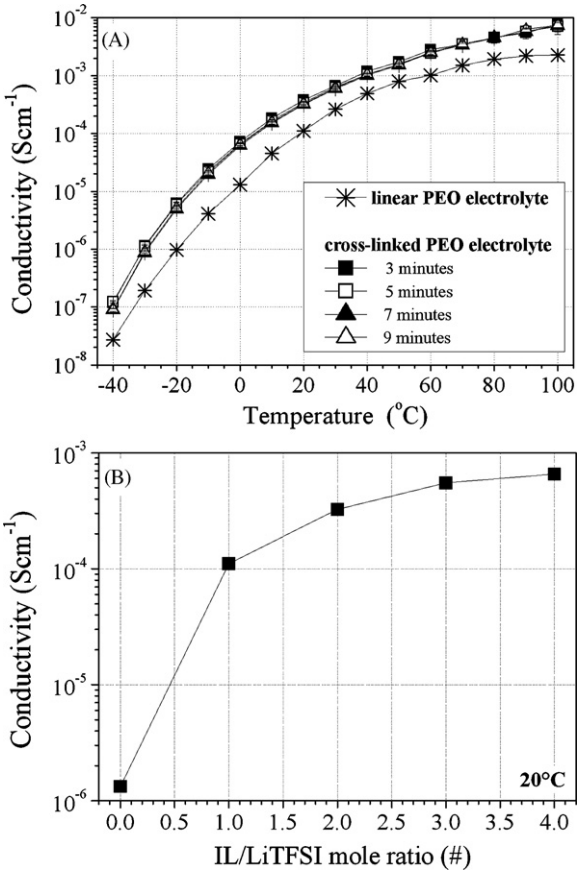

Fig. 4. Ionic conductivity dependence of cross-linked PEO–LiTFSI–PYR_{14}TFSI ternary polymer electrolytes as a function of the temperature (panel A) and the IL/LiTFSI mole ratio at 20 °C (UV photo-irradiation time: 9 min) (panel B). The samples with EO:LiTFSI:PYR_{14}TFSI molar composition of 10:1:1 and 10:1:0 were not cross-linked.

chain fragmentation upon UV photo-irradiation could be excluded because all samples behave uniformly.

3.5. Li/solid polymer electrolyte interface investigation

Li/SPE/Li cells stored at different temperatures have been investigated using impedance measurements in the frequency range extending from 65 kHz to 0.1 Hz (see Fig. 6). All spectra show a slightly depressed semicircle as main feature followed, in the spectra taken at higher temperature, by the typical Li-cation diffusion spur (45° angle) [23]. The first (high frequency) intercept with the real-axis presents the electrolyte resistance (R_{el}) while the second (low frequency) intercept refers to the interfacial resistance (R_{int}), which includes the charge transfer and the passive layer resistances [23]. The comparison of the high frequency intercepts in Fig. 6B reveals a very time stable electrolyte resistance at both investigated temperatures. In particular, the spectra taken at 20 °C show that R_{el} changes only a few Ω over 150 days including an intermediate thermal cycle at 80 °C. This evidence supports for very good chemical and thermal stabilities of the electrolyte since neither extensive reaction with metallic lithium nor thermal decomposition are detected during about 40 days storage at 80 °C. In addition, it indicates a good mechanical stability even at high temperature considering that the polymer electrolyte is hosted in a pouch cell under vacuum, i.e., it is subjected to a constant pressure of 1 kg cm^{-2}.

The interfacial resistance (R_{int}), however, is seen to increase on aging (Table 1), this indicating that a passive layer (also called SEI, Solid Electrolyte Interphase, in liquid electrolyte batteries) [23] is

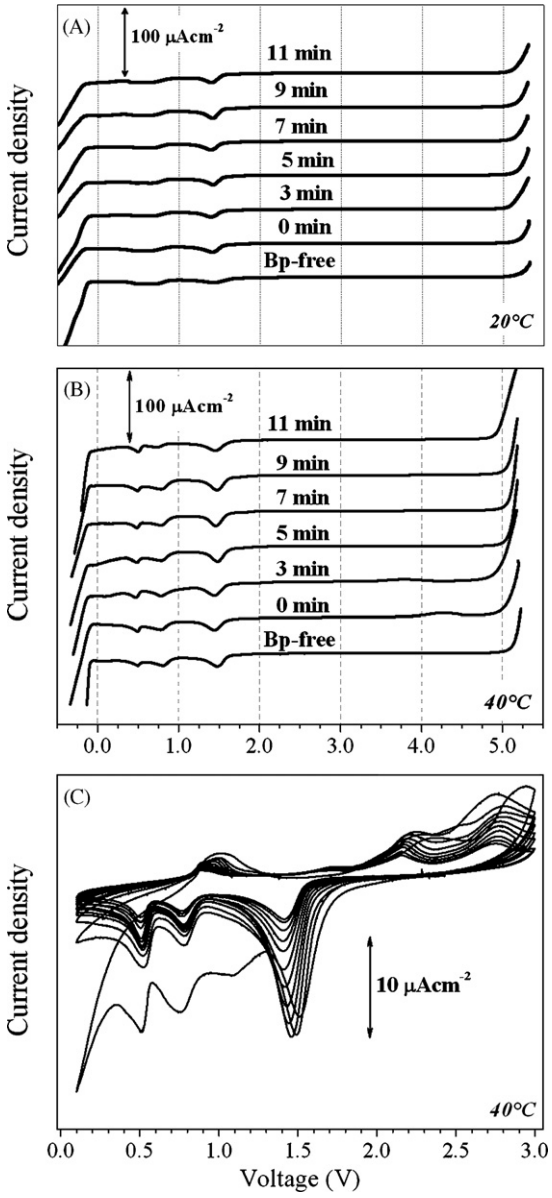

Fig. 5. Electrochemical stability window of cross-linked PEO–LiTFSI–PYR_{14}TFSI ternary polymer electrolytes at 20 °C (panel A) and 40 °C (panel B). The electrolyte samples were processed at different UV photo-irradiation times (see legend). The voltammetric curves of the initiator-free polymer electrolyte are reported for comparison purpose. In panel C are reported consecutive CV curves performed on the sample photo-irradiated for 7 min. W.E.: Ni°; C.E. and R.E.: Li°. Scan rate: 0.5 mV s^{-1}.

formed at the Li/SPE interface. This effect is better observed in Fig. 7 where the evolution of the interfacial resistance of symmetric Li cells, made with several polymer electrolytes differing for the crosslinking time, is reported upon storage at different temperatures. From the figure it is seen that the growth of the passive layer at the Li/SPE interface is, at least initially, not much affected by the UV irradiation time. However, the storage period at 80 °C causes a differentiation of the behavior with the material subjected to the intermediate UV photo-irradiation time showing the better performance (i.e., the lowest increase of R_{int}). Upon lowering the test temperature down to 20 °C, differences between the samples are still observed. In addition, the values of R_{int} are always higher than in the first storage period at 20 °C thus indicating that the storage at 80 °C induces a further growth of the passive interfacial layer.

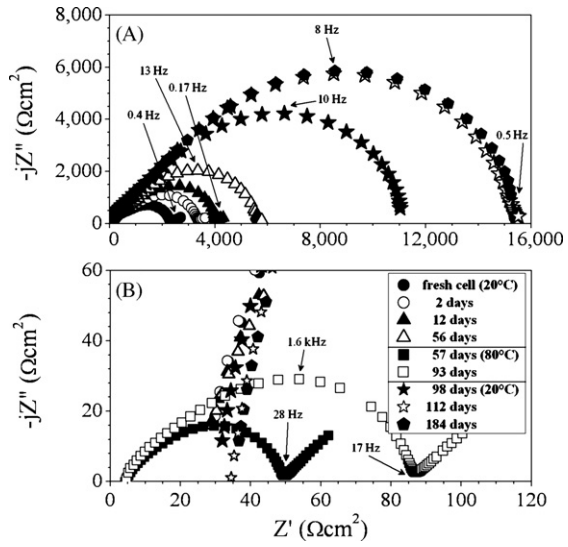

Fig. 6. AC response of a Li/cross-linked PEO–LiTFSI–PYR_{14}TFSI/Li cell at different storage times and temperatures (see legend). The data refer to the cross-linked polymer electrolyte UV photo-irradiated for 9 min. Panel B is a magnification to better show the AC responses recorded at high temperature.

3.6. Lithium plating-stripping tests

Plating-stripping experiments performed on a symmetrical cell with Li-metal electrodes at 40 °C are presented in Fig. 8. The results prove the excellent behavior of the cross-linked ternary polymer electrolyte. After 25 cycles characterized by a decreasing cell overvoltage, most likely due to a partial disruption of the spontaneously formed passive layer, the cell performed very reversibly for up to 1000 cycles. An AC impedance measurement was taken after 1000 cycles and is reported in Fig. 8B. The shape of the impedance response does not show any substantial change with respect to that of a pristine cell (see Fig. 8A). The R_{int} has still a value of $1100 \pm 80\ \Omega$ within the practicable range. The low frequency spur, associated with the Warburg impedance, has a slope of exactly 45° thus indicating a smooth Li surface without major dendritic growth or mossy lithium, which would cause the angle depression. This is highly remarkable after 1000 plating-stripping cycles.

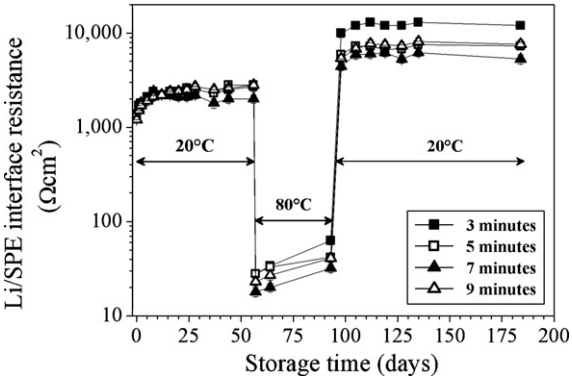

Fig. 7. Time evolution of the interfacial resistance of cross-linked PEO–LiTFSI–PYR_{14}TFSI ternary polymer electrolytes in contact with lithium metal electrodes. The electrolyte samples were processed with different UV photo-irradiation times (see legend). The interfacial resistance is normalized with respect to the lithium electrode active area.

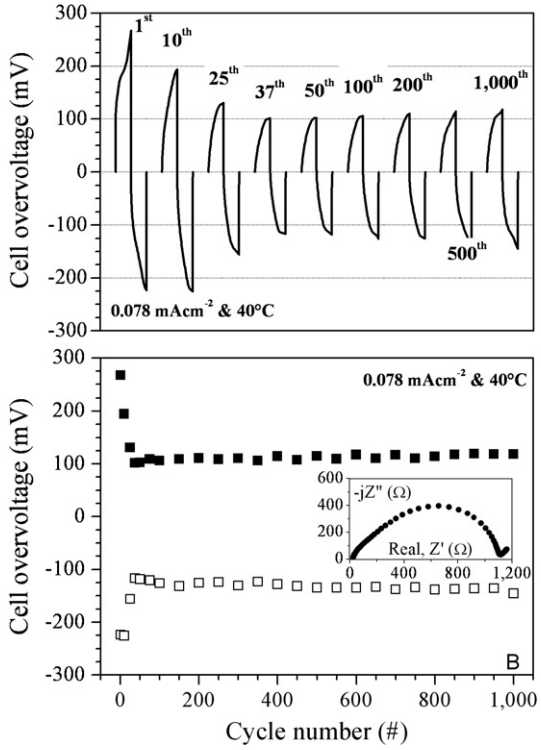

Fig. 8. Selected plating-stripping cycles (panel A) and overvoltage evolution (panel B) measured at the end of each semi cycle during the cycling of a symmetric Li/cross-linked PEO–LiTFSI–$PYR_{14}TFSI$/Li cell at 40 °C (±1 °C). The polymer electrolyte sample under test was UV photo-irradiated for 7 min. Current density: 0.078 mA cm^{-2}. Plating and stripping time: 1 h. Lithium electrode: area: 0.64 cm^2; thickness: 0.05 mm. The insert in panel B depicts the result of AC impedance measurements taken on the cell after 1000 cycles.

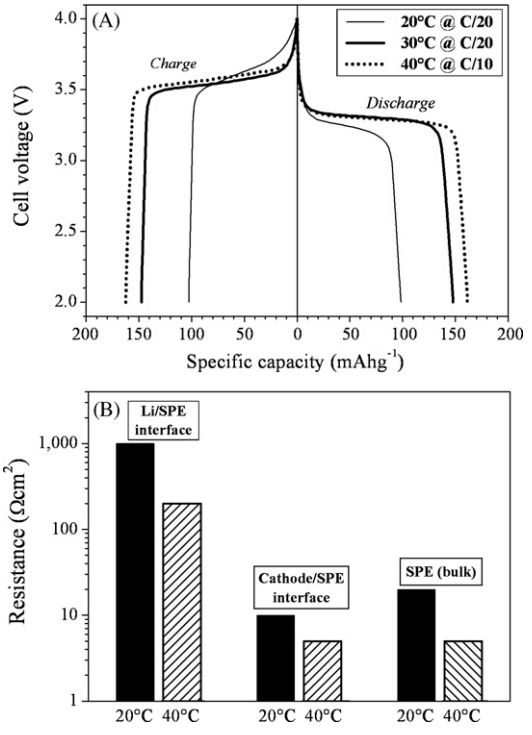

Fig. 9. Voltage vs. capacity profile (panel A) recorded during charge–discharge cycles of Li/cross-linked PEO–LiTFSI–$PYR_{14}TFSI$/$LiFePO_4$ full polymer batteries tested at 20 °C, 30 °C and 40 °C. Panel B illustrates the contribution to the overall cell impedance at 20 °C and 40 °C as detected by AC impedance measurements. The PEO–LiTFSI–$PYR_{14}TFSI$ (10:1:2) polymer electrolyte UV was photo-irradiated for 7 min. Current density: 0.032 mA cm^{-2} (*C*/20) and 0.064 mA cm^{-2} (*C*/10).

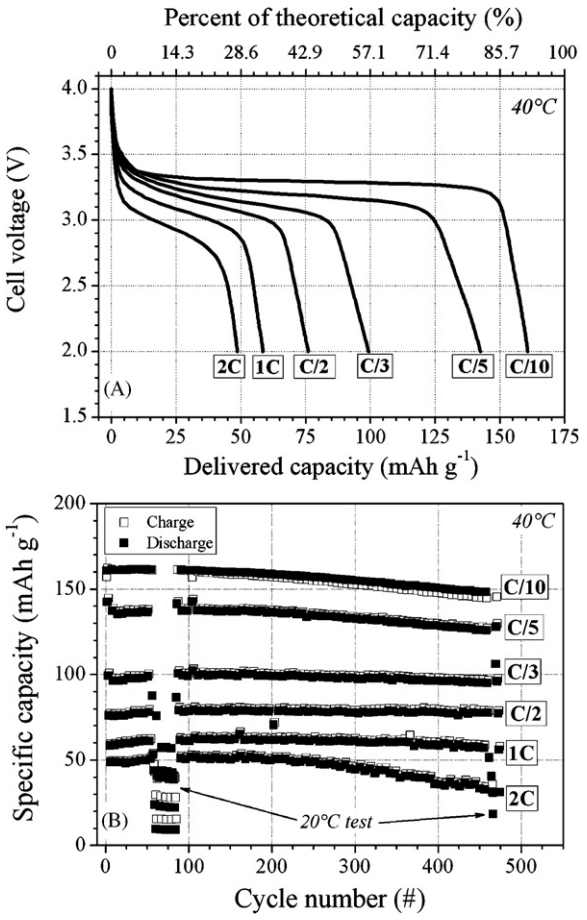

Fig. 10. Voltage vs. capacity profile (panel A) and capacity vs. number of cycles (panel B) of Li/cross-linked PEO–LiTFSI–$PYR_{14}TFSI$/$LiFePO_4$ full polymer batteries tested at 40 °C. The PEO–LiTFSI–$PYR_{14}TFSI$ (10:1:2) polymer electrolyte was UV photo-irradiated for 7 min. Current density: 0.032 mA cm^{-2} (*C*/20); 0.064 mA cm^{-2} (*C*/10); 0.128 mA cm^{-2} (*C*/5); 0.213 mA cm^{-2} (*C*/3); 0.320 mA cm^{-2} (*C*/2); 0.640 mA cm^{-2} (1*C*); 1.280 mA cm^{-2} (2*C*).

3.7. Battery testing

Li/polymer electrolyte/$LiFePO_4$ cells have been assembled to test the capability of the electrolyte to perform in a real battery configuration. The charge–discharge tests were performed at several *C* rates and temperatures. Fig. 9A shows the cycles recorded at *C*/20 (20 °C and 30 °C) and *C*/10 (40 °C). As one can see from the figure, the charge and discharge plateaus for the cells at 30 °C and 40 °C are well defined and the capacities reach 150 mAh g^{-1} and 164 mAh g^{-1}, respectively. As expected because of the high value of the lithium/polymer electrolyte interfacial resistance (R_{int}), the cell tested at 20 °C did not perform as well, even if the capacity approaches 100 mAh g^{-1}. Fig. 9B shows the separated impedance contributions to the overall cell impedance at 20 °C and 40 °C. From the figure it is clear as the cell performance is mostly limited by the resistance at the Li/polymer electrolyte interface at both temperatures but, in particular, at 20 °C.

Fig. 10 reports the combined rate performance and cycle performance test of a Li/SPE/$LiFePO_4$ cell at 40 °C. Panel A presents that the cell was able to deliver more than 100 mAh g^{-1} at *C*/3 rate and about 50 mAh g^{-1} at 2C. Although these values appear to be low when compared with conventional Li-ion battery performance, it should be noted that they are astonishingly high for all-solid-state LMPBs. In addition, these lab-scale cells show very good cycle performance, too (see Fig. 10B). More than 450 cycles were achieved with only a slightly performance decay recorded at the lowest and

the highest rates. The reason of such a behavior is most likely due to the degradation of the active material that is evidenced at the lowest rates by the use of its full capacity and at the highest rates by the use of only the external layer, which, most likely, is the most degraded. The decrease of the operating temperature down to 20 °C (see legend in panel B) results in a decay of the performance that, however, is restored by increasing the temperature to 40 °C.

4. Conclusions

UV cross-linked PEO–LiTFSI–PYR_{14}TFSI solid polymer electrolytes were prepared with a solvent-free procedure and thoroughly characterized in terms of thermal properties, conductivity, electrochemical stability, interfacial properties with lithium metal and battery performance. Except for the cross-linking fraction, no practical difference was observed for polymer electrolytes irradiated for different UV photo-irradiation times.

The electrochemical and mechanical properties of the cross-linked polymer electrolytes showed a great improvement when compared with our previous attempts on these ternary systems [16]. The PEO–LiTFSI–PYR_{14}TFSI solid polymer electrolyte showed conductivities of 3×10^{-4} S cm^{-1} at 20 °C and 10^{-3} S cm^{-1} at 40 °C. The interfacial resistance of the electrolyte in contact with metallic lithium in open circuit condition was found to be rather stable (3000 Ω cm^{-2} at 20 °C and 60 Ω cm^{-2} at 80 °C) upon several months of storage.

Preliminary battery tests in real lithium metal polymer battery (Li/SPE/$LiFePO_4$) have been performed. Charge and discharge tests at a *C*/20 rate yielded more than 100 mAh g^{-1} at 20 °C, 150 mAh g^{-1} at 30 °C and 164 mAh g^{-1} at 40 °C at a *C*/10 rate thus indicating that these batteries are applicable at temperatures higher than 30 °C. The high Li/SPE interfacial resistance at lower temperatures is still a problem. Further work is needed to reduce this matter by, for example, modifying the chemistry of the lithium metal electrode and/or the ionic liquid in order to obtain a thinner and less resistive passive layer at the interface between the electrode and the polymer electrolyte. Nevertheless, the batteries showed very good long-term performance in prolonged, multiple *C*-rate, charge–discharge tests at 40 °C.

Acknowledgements

The authors wish to thank the financial support of the European Commission within the FP6 STREP Project ILLIBATT (Contract no. NMP3-CT-2006-033181). Süd Chemie is acknowledged for kindly providing the $LiFePO_4$ material.

References

[1] C.-H. Doh, D.-H. Kim, H.-S. Kim, H.-M. Shin, Y.-D. Jeong, S.-I. Moon, B.-S. Jin, S.W. Eom, H.-S. Kim, K.-W. Kim, D.-H. Oh, A. Veluchamy, J. Power Sources 175 (2007) 881–885.
[2] D. Fenton, J. Parker, P. Wright, Polymer 14 (1973) 589.
[3] J.-H. Shin, W.A. Henderson, S. Passerini, J. Electrochem. Soc. 152 (2005) A978–A983.
[4] D. Baril, C. Michot, M. Armand, Solid State Ionics 94 (1997) 35–47.
[5] C. Berthier, W. Gorecki, M. Minier, M.B. Armand, J.M. Chabagno, P. Rigaud, Solid State Ionics 11 (1983) 91–95.
[6] R.C. Agrawal, R.K. Gupta, J. Mater. Sci. 34 (1999) 1131–1162.
[7] H.N.W. Lekkerkerker, W.C.K. Poon, P.N. Pusey, A. Stroobants, P.B. Warren, Europhys. Lett. 20 (2004) 559–564.
[8] J.-H. Shin, W.A. Henderson, S. Passerini, Electrochem. Commun. 5 (2003) 1016–1020.
[9] K.E. Johnson, Electrochem. Soc. Interface 16 (2007) 38–41.
[10] Q. Zhou, W.A. Henderson, G.B. Appetecchi, J. Phys. Chem. B (2008) 13577–13580.
[11] S. Randstrom, M. Montanino, G.B. Appetecchi, C. Lagergren, A. Moreno, S. Passerini, Electrochim. Acta 53 (2008) 6397–6401.
[12] S. Randstroem, G.B. Appetecchi, C. Lagergren, A. Moreno, S. Passerini, Electrochim. Acta 53 (2008) 1837–1842.
[13] G.B. Appetecchi, S. Scaccia, C. Tizzani, F. Alessandrini, S. Passerini, J. Electrochem. Soc. 153 (2006) A1685–A1691.
[14] W.A. Henderson, S. Passerini, Chem. Mater. 16 (2004) 2881–2885.
[15] I. Nicotera, C. Oliviero, W.A. Henderson, G.B. Appetecchi, S. Passerini, J. Phys. Chem. B (2005) 22814–22819.
[16] M. Castriota, T. Caruso, R.G. Agostino, E. Cazzanelli, W.A. Henderson, S. Passerini, J. Phys. Chem. A 109 (2005) 92–96.
[17] J.-M. Tarascon, M. Armand, Nature 414 (2001) 359–367.
[18] J.-H. Shin, W.A. Henderson, G.B. Appetecchi, F. Alessandrini, S. Passerini, Electrochim. Acta 50 (2005) 3859–3865.
[19] G.-T. Kim, G.B. Appetecchi, F. Alessandrini, S. Passerini, J. Power Sources 171 (2007) 861–869.
[20] B. Rupp, M. Schmuck, A. Balducci, M. Winter, W. Kern, Eur. Polym. J. 44 (2008) 2986–2990.
[21] B.A. Boukamp, Solid State Ionics 18–19 (1986) 136–140.
[22] B.A. Boukamp, Solid State Ionics 20 (1986) 31–44.
[23] J.R. MacDonald, Impedance Spectroscopy, John Wiley & Sons Editor, New York, 1987.
[24] A.J. Nijenhuis, E. Colstee, D.W. Grijpma, A.J. Pennings, Polymer 37 (1996) 5849–5857.
[25] W.A. Henderson, S. Passerini, Electrochem. Commun. 5 (2003) 575–578.
[26] W. Gorecki, C. Roux, M. Clemancey, M. Armand, E. Belorizky, Chem. Phys. Chem. 7 (2002) 620–625.
[27] G.B. Appetecchi, W. Henderson, P. Villano, M. Berrettoni, S. Passerini, J. Electrochem. Soc. 148 (2001) A1171–A1178.
[28] J.-H. Shin, W.A. Henderson, C. Tizzani, S. Passerini, S.S. Jeong, K.-W. Kim, J. Electrochem. Soc. 153 (2006) A1649–A1654.
[29] H. Vogel, Phys. Z. 22 (1921) 645;
G.S. Fulcher, J. Am. Chem. Soc. 8 (1925) 339;
G. Tamman, W. Hesse, Z. Anorg. Allg. Chem. 156 (1926) 245.
[30] S. Passerini, B. Scrosati, J. Electrochem. Soc. 141 (1994) 889–895.